Biochemical and Biophysical Research Communications 433 (2013) 432–437

Contents lists available at SciVerse ScienceDirect

Biochemical and Biophysical Research Communications

journal homepage: www.elsevier.com/locate/ybbrc

Generation of reactive oxygen species by a novel berberine–bile acid analog mediates apoptosis in hepatocarcinoma SMMC-7721 cells

Qingyong Li *, Li Zhang, Yuangang Zu, Tianyu Liu, Baoyou Zhang, Wuna He

Key Laboratory of Forest Plant Ecology (Northeast Forestry University), Ministry of Education, China

ARTICLE INFO

Article history:
Received 3 February 2013
Available online 19 March 2013

Keywords:
A novel berberine–bile acid analog
Reactive oxygen species
SMMC-7721
Apoptosis

ABSTRACT

2,3-Methenedioxy-9-*O*-(3′α,7′α-dihydroxy-5′β-cholan-24′-propy-lester)berberine (**B4**) is a novel berberine–bile acid analog synthesized in our laboratory. Previously, we showed that **B4** exerted greater cytotoxicity than berberine in several human cancer cell lines. Therefore, we further evaluated the mechanism governing its anticancer actions in hepatocellular carcinoma SMMC-7721 cells. **B4** inhibited the proliferation of SMMC-7721 cells, and stimulated reactive oxygen species (ROS) production and mitochondrial membrane depolarization; anti-oxidant capacity was reduced. **B4** also induced the release of cytochrome *c* from the mitochondria to the cytosol and an increase in poly ADP-ribose polymerase (PARP) cleavage products, reflective of caspase-3 activation. Moreover, **B4** induced the nuclear translocation of apoptosis-inducing factor (AIF) and a rise in DNA fragmentation. Pretreatment with the anti-oxidant *N*-acetylcysteine (NAC) inhibited **B4**-mediated effects, including cytotoxicity, ROS production, mitochondrial membrane depolarization increase in intracellular Ca^{2+}, cytochrome *c* release, PARP cleavage, and AIF translocation. Our data suggest that **B4** induces ROS-triggered caspase-dependent and caspase-independent apoptosis pathways in SMMC-7721 cells and that ROS production may be a specific potential strategy for treating hepatic carcinoma.

1. Introduction

Berberine (Fig. 1A), an isoquinolone quaternary alkaloid isolated from the root and bark of *Berberis aristata* or *Coptis chinensis*, has been extensively used as a non-prescription drug to treat diarrhea since the 1950s and has continuously had good safety records in clinical applications [1–3]. Recent studies have demonstrated that berberine inhibits the growth of various tumor cell types, including liver, lung, oral, bladder, breast, and prostate [4]. Multiple mechanisms have been reported for berberine-induced apoptosis, depending on the cell type: G1 phase cell cycle arrest in prostate cancer (DU145, PC-3, and LNCaP) cells, induction of mitochondria-dependent apoptosis in human breast cancer (MCF-7) cells, and death receptor and mitogen-activated protein kinase (MAPK) pathways in HeLa cells [5–7]. Berberine has also been shown to reduce melanoma cell (A375 and Hs294) migration by reducing the expression of COX-2, PGE2 and its receptor [8].

Although stable in the gastrointestinal tract, berberine is poorly absorbed in the intestine, resulting in insufficient plasma concentrations and low efficacy [9]. Because bile acids are transported across cell membranes by active transport, they represent a possible targeting vector to improve bioavailability [10]. Therefore, we synthesized a novel berberine–bile acid analog, 2,3-methenedioxy-9-*O*-(3′α,7′α-dihydroxy-5′β-cholan-24′-propy-lester) berberine (**B4**) (Fig. 1B). Previous studies in our laboratory have shown that **B4** has improved oral bioavailability in mice and increased cytotoxicity toward several human cancer cell lines, including SGC-7901 (gastric), HCT-116 (colon), SMMC-7721 (hepatocellular), and BEL-7402 (hepatocellular). **B4** was most effective against SMMC-7721, indicating the liver-specificity of bile acids [11].

Caspase-dependent apoptosis can occur by one of two representative pathways: the death receptor-mediated (extrinsic) pathway and the mitochondrial (intrinsic) pathway. The extrinsic pathway is initiated by the binding of death ligands to cell surface receptors, causing subsequent caspase-8 activation [12]. The intrinsic pathway involves the efflux of cytochrome *c* from mitochondria to the cytosol, where it subsequently forms a complex (apoptosome) with Apaf-1 and caspase-9, leading to caspase-3 activation [13]. An alternative apoptotic pathway is the caspase-independent pathway involving the apoptosis-inducing factor (AIF) and endonuclease G (EndoG) [14,15]. AIF, located in the mitochondrial intermembranous space, is released from the mitochondria and is translocated to the nucleus where it induces chromatin condensation and DNA fragmentation [16]. Additionally, reactive oxygen species (ROS) cause mitochondrial dysfunction, which may cause cell apoptosis [17].

* Corresponding author. Address: 332# No. 26 Hexing Road, Harbin City 150040, Heilongjiang Province, China. Fax: +86 451 82102082.
E-mail address: li_qingyong@126.com (Q. Li).

0006-291X/$ - see front matter Crown Copyright © 2013 Published by Elsevier Inc. All rights reserved.
http://dx.doi.org/10.1016/j.bbrc.2013.02.104

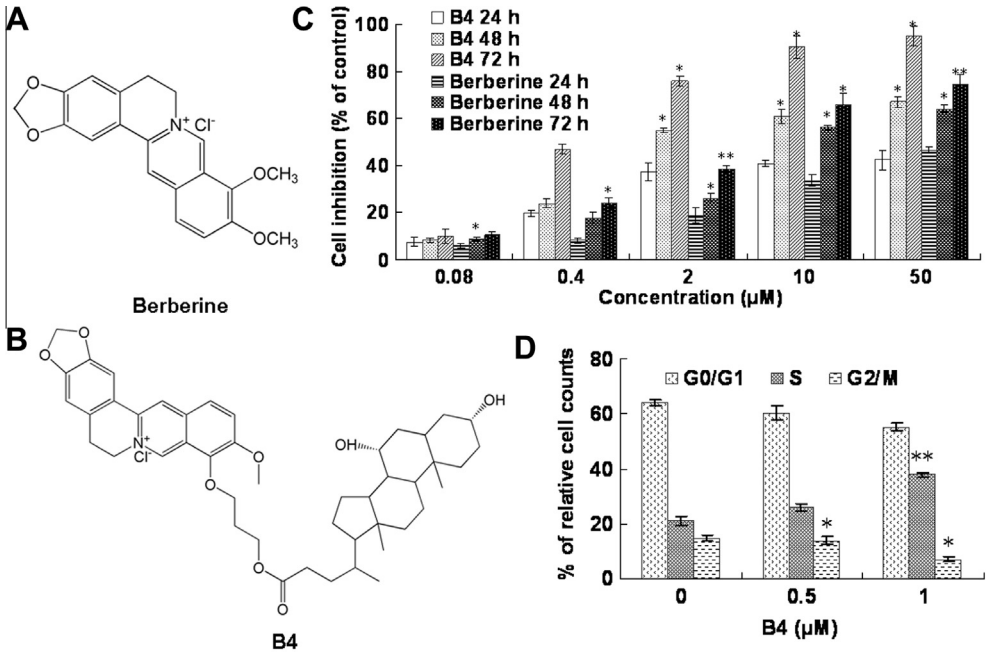

Fig. 1. The chemical structures of: (A) berberine and (B) **B4**. (C) Effect of **B4** on cell proliferation. SMMC-7721 cells were incubated with 0, 0.08, 0.4, 2, 10, or 50 μM **B4** or berberine for 24, 48, or 72 h; inhibition of cell proliferation was measured using an MTT assay. Values were calculated as % proliferation inhibition compared to control. (D) Effect of **B4** on cell cycle distribution of SMMC-7721 cells. The results were analyzed by Mod Fit LT 3.0. Each experiment was performed in triplicate. $^{*}p < 0.05$, $^{**}p < 0.01$ vs. control, which was treatment with DMSO.

Here, we demonstrate the mechanisms by which **B4** exerts its anticancer actions in SMMC-7721 cells. We found that **B4** activates caspase-dependent and caspase-independent apoptosis pathways, and those related to ROS production. These data suggest that regulation of ROS generation may be a strategy for treating hepatic carcinoma that is resistant to pro-apoptotic therapeutics.

2. Materials and methods

2.1. Chemicals and reagents

Chemicals and reagents used in this study are listed in Supplementary data.

2.2. Cell culture

SMMC-7721 cells and normal human liver HL-7702 cells were obtained from the Cell Bank of Shanghai Institute of Biochemistry and Cell Biology, Chinese Academy of Sciences (Shanghai, China). SMMC-7721 cells and HL-7702 cells were maintained in RPMI-1640 containing 10% FBS and 1% penicillin/streptomycin and cultured at 37 °C in a 5% CO_2 incubator. **B4** and berberine were initially dissolved in DMSO, and were made up in culture medium before each experiment. Unless otherwise mentioned, control cells were treated with an equal amount of DMSO. The maximum amount of DMSO was maintained at less than 0.1% v/v and was nontoxic to the cells.

2.3. Cell proliferation assay

SMMC-7721 or HL-7702 cells (1×10^6 cells/well) were either untreated or treated with different concentrations (0.8–50 μM) of **B4** or berberine for 24, 48 or 72 h. Cell proliferation was measured by the MTT assay using DMSO to dissolve formazan as mentioned previously [18].

2.4. Cell cycle analysis and apoptosis assays

SMMC-7721 cells were plated in 6-well plates (1×10^6 cells/well) and incubated with 0, 0.5, or 1 μM **B4** for 48 h. Cells were then harvested by centrifugation. Cell pellets were re-suspended in PBS (800 μL) and stained with CyStain (200 μL) for 10 min in the dark. The cell cycle distribution was analyzed by flow cytometry (Partec GmbH, Germany).

Phosphatidylserine exposed on the outside of the apoptotic cells was determined by the Annexin V-FITC Apoptosis Kit according to the manufacturer's instructions. SMMC-7721 cells were plated in 6-well plates (1×10^6 cells/well) and incubated with **B4** or berberine for 48 h. Cells were harvested and gently re-suspended in Annexin V-FITC binding buffer (195 μL) plus Annexin V-FITC (5 μL) for 10 min at in the dark. Cells were then centrifuged at 3000*g* for 5 min and gently re-suspended in Annexin V-FITC binding buffer (190 μL) and propidium iodide (10 μL), followed by immediate analysis by flow cytometry.

2.5. Determination of DNA fragmentation

SMMC-7721 cells were either untreated or treated with **B4** (0.5, 1, or 2 μM) or berberine (1 or 2 μM) for 48 h. Apoptotic DNA Ladder Detection Kit was used to extract DNA fragments from cells according to the manufacturer's instructions. The extracted DNA samples were electrophoresed in a 1.5% agarose gel and stained with ethidium bromide in the dark at 37 °C for 1 h. Gel images were captured using a UV-transilluminator (Fuji Life Science, Irvine, CA, USA).

2.6. Detection of ROS

Intracellular ROS production was measured using the Reactive Oxygen Species Assay Kit according to the manufacturer's instructions. Cells were either untreated or treated with **B4** (2 μM) for 48 h in the absence or presence of 5 mM NAC; NAC was added 1 h prior to **B4**. Cells were collected and re-suspended in 10 μM

2,7-dichlorodihydrofluorescein diacetate (DCFH-DA). After incubation for 20 min at 37 °C in the dark, cells were analyzed for fluorescence intensity by flow cytometry; ROS levels were quantified with WinMDI 2.8 software.

2.7. Measurement of mitochondrial membrane potential ($\Delta\Psi$ m) and intracellular Ca^{2+} levels

SMMC-7721 cells (1×10^6 cells/well) were incubated with 2 μM **B4** for 48 h in the absence or presence of 5 mM NAC; NAC was added 1 h prior to **B4**. $\Delta\Psi$ m was monitored by measuring the uptake of a mitochondria specific dye, rhodamine-123 (Rh-123). Cells were washed and harvested in PBS containing Rh-123 (10 μg/mL) for 30 min at 37 °C; cells were analyzed immediately by flow cytometry. Separately, the intracellular Ca^{2+} concentration was measured using the fluorescent indicator Fluo-3/AM. Fluo-3/AM (10 μL) was added for 30 min at 37 °C in the dark. The samples were re-suspended in PBS and analyzed immediately by flow cytometry. $\Delta\Psi$ m and intracellular Ca^{2+} levels were quantified with WinMDI 2.8 software.

2.8. Protein extraction and Western blot analysis

After incubation with 0, 0.5, 1, or 2 μM **B4** for 48 h, SMMC-7721 cells were collected and lysed with ice-cold lysis buffer containing 1% phenylmethylsulfonyl fluoride (PMSF). Cytochrome *c* and AIF released from mitochondria were detected using the Nuclear and Cytoplasmic Protein Extraction Kit. The protein concentration was determined using the BCA Protein Assay Kit. Protein samples were separated by 8% or 12% SDS–PAGE and transferred to a polyvinylidene fluoride (PVDF) membrane using a semi-dry transfer. Membranes were incubated with different monoclonal antibodies overnight at 4 °C and further incubated for 1 h with alkaline phosphatase-conjugated secondary antibodies. Then the membranes were immersed in BCIP/NBT solution until color appeared. The reaction was stopped by the addition of distilled water.

2.9. Statistical analysis

The results are expressed as mean ± SD for triplicate experiments. Statistical significance was determined by one-way analysis of variance (ANOVA) followed by the Bonferroni post hoc test for multiple comparisons or the two-tailed Student's *t*-test. *P*-values less than 0.05 were considered statistically significant.

3. Results

3.1. Effect of *B4* on cell growth inhibition and cell cycle distribution in human hepatoma cells

B4 and berberine caused dose- and time-dependent inhibition of proliferation in SMMC-7721 cells (Fig. 1C). At all doses $\geqslant$0.4 μM, **B4** elicited a greater inhibitory effect than berberine at 72 h. The maximal inhibitory effect (50 μM at 72 h) was significantly greater with **B4** (95.0 ± 4.0%) compared to berberine (74.7 ± 3.9%). Conversely, berberine exhibited a greater cytotoxic effect on normal human liver cells (HL-7702) at all doses $\geqslant$0.4 μM compared to **B4**. In all subsequent experiments, 2 μM **B4** was the highest concentration used since it inhibited proliferation of normal cells by <20% after 48 h (Supplementary Fig. S1). **B4** suppressed the growth of SMMC-7721 cells and morphological changes also indicated that **B4** treatment decreased cell density and increased the numbers of floating cells (data not shown), which indicated that the observed growth inhibition was due to cell death.

Previously, berberine treatment arrested the cell cycle of SMMC-7721 cells at the sub-G1 phase [19]. However, after SMMC-7721 cells treatment with **B4**, the percent of cells at S phase was increased from 21.15 to 37.75% and the percent of cells at G0/G1 phase and G2/M phase were reduced in a dose-dependent manner. **B4** induced the accumulation of SMMC-7721 cells at S phase (Fig. 1D).

3.2. *B4* induces more significant apoptosis in human hepatoma SMMC-7721 cells than berberine

Flow cytometry analysis of double-stained SMMC-7721 cells – Annexin V (to detect the exposed phospholipid membrane components of apoptotic cells) and PI (to detect nonviable cells) – was used to quantify apoptotic changes. As shown in Fig. 2A and B, the percentage of total apoptotic cells (Annexin V+) increased significantly with increasing concentration of **B4** (from 5.29 ± 0.8% to 59.52 ± 2.8%), but not with berberine.

DNA fragmentation into nucleosomes containing 180–200 bp or multiples of 200 bp is one of the hallmarks of apoptosis [20]. **B4** treatment led to the appearance of ladder-like strips regardless of the concentration used (Fig. 2C). Untreated cells and those treated with berberine did not exhibit DNA fragmentation. These data suggest that **B4** inhibited cell proliferation by triggering apoptotic cell death in SMMC-7721 cells.

3.3. *B4* triggers caspase-dependent and caspase-independent apoptosis pathway in SMMC-7721 cells

Activation of the caspase cascade is another hallmark of apoptosis. Cytochrome *c* released from mitochondria into the cytosol triggers the formation of the apoptosome, resulting in the activation of caspases [21]. Fig. 2D shows that levels of procaspases-3, -8, and -9 were reduced in a dose-dependent manner. As confirmation of caspase-3 activation, we detected a rise in the cleavage fragment of the caspase-3 substrate poly (ADP-ribose) polymerase (PARP) with increasing concentrations of **B4**. **B4** also caused a dose-dependent decrease in the level of the X-lined inhibitor of apoptosis (XIAP) protein, a member of the inhibitor of apoptosis (IAP) family that selectively binds and inhibits caspases-3 and -9. Additionally, **B4** caused a dose-dependent increase and decrease of cytosolic and mitochondrial cytochrome, respectively (Fig. 2E). Together, these results suggest the involvement of the caspase pathway in **B4**-induced apoptosis in SMMC-7721 cells.

We also examined activation of caspase-independent pathways by **B4**. Apoptosis-inducing factor (AIF) has been identified as an apoptogenic mitochondrial intermembrane protein that translocates to the nucleus and triggers DNA fragmentation [16]. AIF translocated from mitochondria to the nucleus in a dose-dependent manner. Moreover, **B4** up- and down-regulated the expression of Bax and Bcl-2, respectively, leading to an increase in the Bax/Bcl-2 ratio, an important marker of apoptosis in cancer cells (Fig. 2F).

3.4. *B4*. induces ROS generation in SMMC-7721 cells

SMMC-7721 cells were treated with 2 μM **B4** for 48 h in the presence or absence of NAC, a nonspecific ROS scavenger. As shown in Fig. 3A and B, compared with control cells, treatment with 2 μM **B4** for 48 h markedly increased ROS generation. Pretreatment with NAC, significantly blocked the **B4**-mediated rise in ROS. MTT assay showed that cell viability increased from 48.3% ± 2.9% to 79.5% ± 3.1% in the presence of NAC, which suggested that NAC also protected the SMMC-7721 cells from growth inhibition by **B4** (Fig. 3C). Moreover, **B4** reduced intracellular levels of the antioxidant GSH; at 2 μM **B4**, GSH levels decreased to 49% of control

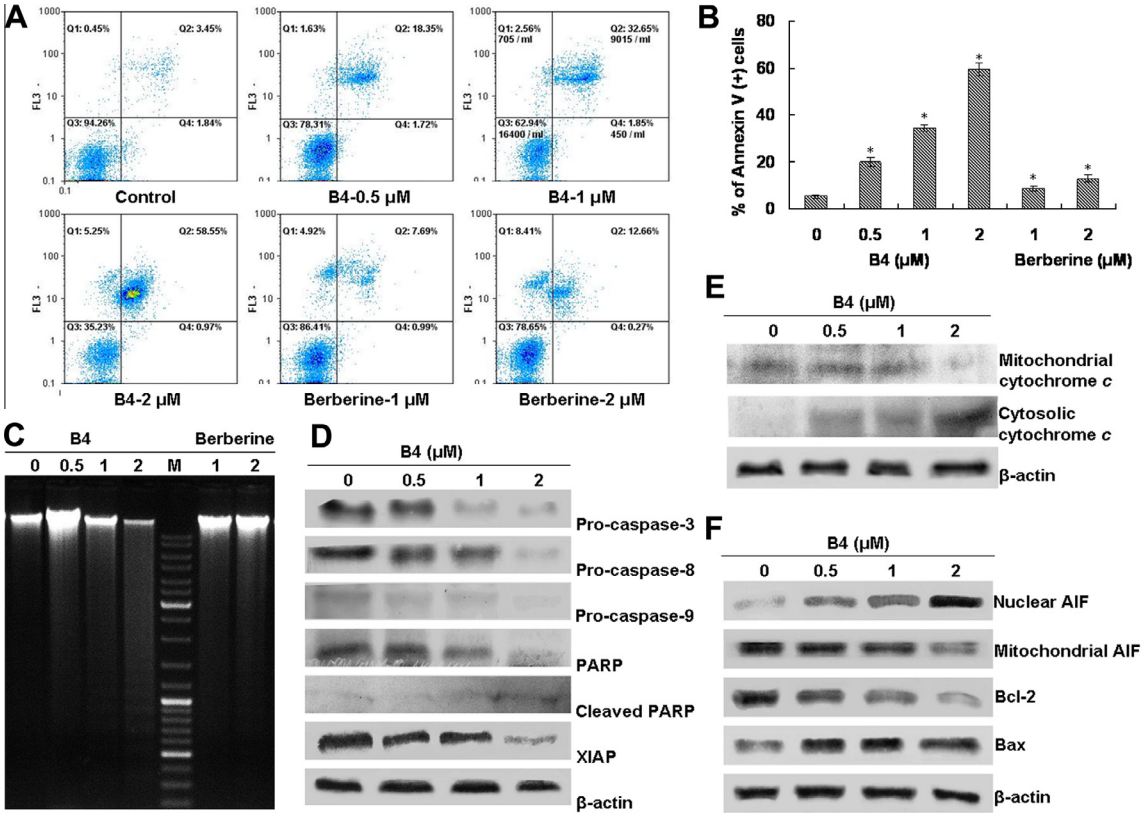

Fig. 2. Apoptotic effect of **B4** on SMMC-7721 cells. SMMC-7721 cells were either untreated or treated with incubated with 0.5, 1, or 2 μM **B4** or 1 or 2 μM berberine for 48 h. (A) Apoptotic population of SMMC-7721 cells analysis by flow cytometric using annexin V-FITC/PI staining. Q1, necrotic cells (annexin V−/PI+); Q2, late apoptotic cells (annexin V+/PI+); Q3, viable cells (annexin V−/PI−); Q4, early apoptotic cells (annexin V+/PI−). The percentage of Annexin V-positive population in panel (B) indicates induction of apoptosis cells at every concentration of **B4**. $^{*}p < 0.05$ vs. control (0 μM). (C) DNA fragmentation of **B4**-induced apoptosis was detected using 1.5% agarose gel electrophoresis. M indicates marker for DNA size. (D–F) Modulation of expression of caspase-dependent and caspase-independent apoptosis-related proteins by **B4** in SMMC-7721 cells. β-Actin was used as an internal control. PARP = poly (ADP-ribose) polymerase; XIAP = X-lined inhibitor of apoptosis; AIF = apoptosis-inducing factor.

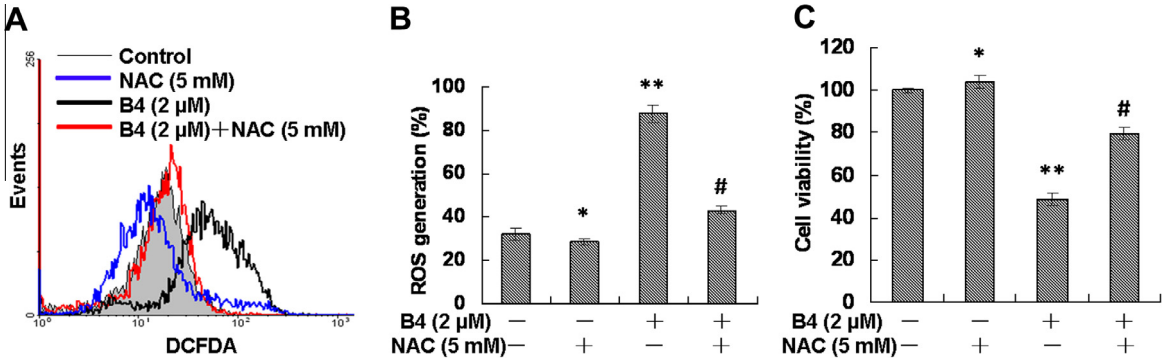

Fig. 3. Effect of anti-oxidant pretreatment on **B4**-mediated effects. SMMC-7721 cells were either untreated or treated with **B4** (2 μM) in the absence or presence of *N*-acetylcysteine (NAC; 5 mM) for 48 h. (A and B) Production of reactive oxygen species (ROS) was measured by flow cytometry. In panel B, the data represent the percentages of cells within the specified fluorescence intensity range using WinMDI 2.8 software. (C) Cell viability was examined by MTT assay. $^{*}p < 0.05$ and $^{**}p < 0.01$ vs. control (0 μM), $^{\#}p < 0.05$ vs. **B4**-treated cells (2 μM).

(Supplementary Fig. S2). Together, these data suggest ROS generation plays an essential role in the growth inhibition activity of **B4** in SMMC-7721 cells.

3.5. ROS triggered *B4*-induced cell caspase-dependent and caspase-independent apoptosis

Excessive levels of ROS are reported to cause mitochondrial dysfunction leading to a loss of mitochondrial membrane potential ($\Delta\Psi$ m) and an increase in intracellular Ca^{2+}; disruption of $\Delta\Psi$ m is one of the earliest intracellular events in apoptosis induction, and this reduction in $\Delta\Psi$ m is often accompanied by the production of ROS [18,22]. As shown in Fig. 4A and B, **B4** elicited a significant increase in intracellular Ca^{2+}, an important messenger molecule in apoptosis; pretreatment with NAC decreased the Ca^{2+} level to that of control. **B4** also reduced the fluorescence intensity in Rh-123-loaded cells, reflecting a decrease in $\Delta\Psi$ m; mitochondrial membrane depolarization was blocked by pretreatment with 5 mM NAC (Fig. 4C), suggesting that **B4**-induced dysfunction of mitochondria is caused by ROS generation.

We also assessed the effects of ROS on the expression of key pro-apoptotic proteins. Western blot analysis showed that

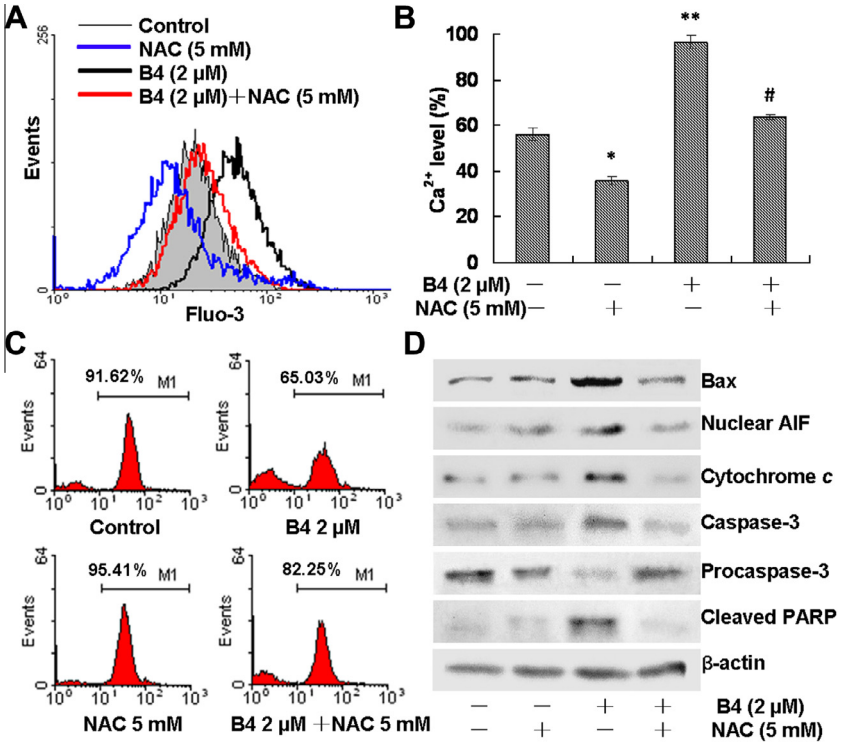

Fig. 4. Effect of ROS on **B4**-induced cell apoptosis. SMMC-7721 cells were either untreated or treated with **B4** (2 μM) in the absence or presence of *N*-acetylcysteine (NAC; 5 mM) for 48 h. (A and B) The level of intracellular Ca^{2+} in SMMC-7721 cells was determined by flow cytometry with Fluo-3/AM. $^{*}p < 0.05$ vs. control (0 μM), $^{\#}p < 0.05$ vs. **B4**-treated cells (2 μM). (C) Changes in mitochondrial membrane potential ($\Delta\psi$ m) were measured by flow cytometry with Rhodamine-123. The numbers in each graph represent the percentages of cells in the M1 gate, which is reflective of a high $\Delta\psi$ m. (D) Effect of **B4** (2 μM) on expression of apoptosis-related proteins was determined in the absence or presence of NAC (5 mM). Total protein was extracted and Bax, caspase-3, poly(ADP-ribose) polymerase (PARP) cleavage products, cytosolic cytochrome *c*, and nuclear AIF were analyzed by Western blot; β-actin was used as an internal control.

pretreatment with NAC protected against cytochrome *c* release and AIF translocation to nucleus. Concomitantly, the expressions of procaspase-3, PARP, and Bax were restored to levels of control cells by NAC treatment (Fig. 4D). These results suggest that NAC exerts cytoprotective effects on **B4**-induced caspase-dependent and caspase-independent apoptosis by suppressing caspase activation, cytochrome *c* release, and AIF translocation.

4. Discussion

China has one of the highest mortality rates associated with hepatocellular carcinoma (HCC), an aggressive cancer with an extremely poor prognosis [23]. The vast majority of HCC is detected at an advanced stage that is highly resistant to conventional chemotherapy, radiation therapy, and even immunotherapy [24]. Adverse effects from these chemotherapy agents may lead to prolonged suffering and even death [25]. Therefore, the development of new therapies that can specifically target cancer cells but with minimal toxicity toward normal cells would be clinically beneficial.

We examined the anti-proliferative and anti-tumor activity of **B4**, a berberine–bile acid conjugate. **B4** caused a dose- and time-dependent inhibition of SMMC-7721 cell proliferation, arrested the cell cycle at S phase, and induced morphological changes associated with cell death. The key findings of the present study are that **B4** elicited a greater growth inhibitory effect on hepatoma cells compared to berberine, and had minimal effect on normal liver (HL-7702) cells.

Activation of caspases by extrinsic and intrinsic pathways plays an essential role in apoptosis. Our results suggest that **B4** stimulates apoptosis through both pathways. Caspase-8 mediates the response downstream of ligand binding to death receptors [12]. Our results showing the disappearance of procaspase-8, and thus presumably the accumulation of caspase-8, with **B4** suggests it may stimulate the extrinsic or death receptor-mediated apoptosis pathway. We also found that **B4** elicited responses associated with activation of the intrinsic pathway. The intrinsic pathway is mediated by release of cytochrome *c* from mitochondria into the cytosol, where it activates procaspase-9 in a complex with Apaf-1; caspase-9 subsequently activates caspase-3 [26]. Treatment with **B4** caused an increase in the cleavage products of the caspase-3 substrate PARP and down-regulated expression of the XIAP, one of the most potent caspase inhibitors.

We found that **B4** also activated caspase-independent apoptosis pathways. Nuclear translocation of AIF represents the primary pathway of caspase-independent cell death signaling. It corresponds with early commitment to apoptosis and is correlated with large-scale DNA fragmentation. In our study, we observed a profound increase of AIF in the nucleus, with a concomitant decline in the mitochondria.

Our results suggest that ROS production plays an important role in **B4**-induced apoptosis. ROS are highly reactive forms of molecular oxygen; mitochondria are a primary source. Excessive levels of ROS, however, cause severe cause severe mitochondrial dysfunction in which breakdown of the functional integrity of the mitochondrial membrane leads to loss of mitochondrial proteins and mitochondrial membrane depolarization [22]. **B4** stimulated ROS production, caused mitochondrial membrane depolarization, and reduced the anti-oxidant capacity by lowering the level of GSH. Moreover, **B4** caused in an increase in cytoplasmic Ca^{2+} and elicited changes in protein levels associated with apoptosis, including increases in Bax, cytoplasmic cytochrome *c*, nuclear-localized AIF, and cleaved PARP products, and decreases in procaspase-3, -8,

and -9. However, pretreatment with the anti-oxidant NAC prevented **B4**-induced apoptosis by inhibiting ROS generation. Furthermore, NAC offered significant protection against **B4**-induced mitochondrial membrane depolarization, cytochrome *c* release, PARP cleavage, procaspase-3 down-regulation, and Bax up-regulation, and AIF translocation. Together, these data suggest that ROS generation is an early event in the process of **B4**-induced apoptosis.

Based on our data, we propose a model by which **B4**-mediated generation of ROS leads to apoptosis (Supplementary Fig. S3). The current study demonstrates that **B4**-induced ROS generation causes an oxidant-antioxidant imbalance and oxidative damage, followed by mitochondrial membrane depolarization, increases in the intracellular Ca^{2+} concentration and in the Bax/Bcl-2 ratio, and loss of mitochondrial proteins. AIF is translocated to the nucleus (caspase-independent apoptosis), leading to DNA fragmentation, while cytochrome *c* is released into the cytosol, where it activates the caspase cascade, as evidence by the increase in cleaved PARP products. This is accompanied by a down-regulation of XIAP. Moreover, activition of caspase-8 suggests that **B4** may act through the extrinsic or death receptor-mediated apoptosis pathway; however, further investigation is warranted.

In conclusion, **B4** has greater anticancer potential than berberine against human hepatocellular carcinoma SMMC-7721 cells. Targeting ROS may be a viable strategy to treat hepatic carcinoma that is resistant to pro-apoptotic therapeutics.

Acknowledgments

The authors gratefully acknowledge the financial support by National Natural Science Foundation of China (31270397).

Appendix A. Supplementary data

Supplementary data associated with this article can be found, in the online version, at http://dx.doi.org/10.1016/j.bbrc.2013.02.104.

References

[1] M. Ikram, A review on the chemical and pharmacological aspects of genus *Berberis*, Planta Med. 28 (1975) 353–358.
[2] C.W. Lau, X.Q. Yao, Z.Y. Chen, et al., Cardiovascular actions of berberine, Cardiovasc. Drug Rev. 19 (2001) 234–244.
[3] X.H. Zeng, X.J. Zeng, Y.Y. Li, Efficacy and safety of berberine for congestive heart failure secondary to ischemic or idiopathic dilated cardiomyopathy, Am. J. Cardiol. 92 (2003) 173–176.
[4] X. Xia, J. Yan, Y. Shen, et al., Berberine improves glucose metabolism in diabetic rats by inhibition of hepatic gluconeogenesis, PLoS One 6 (2011) e16556.
[5] S.K. Mantena, S.D. Sharma, S.K. Katiyar, Berberine, a natural product, induces G1-phase cell cycle arrest and caspase-3-dependent apoptosis in human prostate carcinoma cells, Mol. Cancer Ther. 5 (2006) 296–308.
[6] J.B. Patil, J. Kim, G.K. Jayaprakasha, Berberine induces apoptosis in breast cancer cells (MCF-7) through mitochondrial-dependent pathway, Eur. J. Pharmacol. 645 (2010) 70–78.
[7] B. Lu, M. Hu, K. Liu, et al., Cytotoxicity of berberine on human cervical carcinoma HeLa cells through mitochondria, death receptor and MAPK pathways, and in-silico drug-target prediction, Eur. J. Pharmacol. 645 (2010) 70–78.
[8] T. Singh, M. Vaid, N. Katiyar, et al., Berberine, an isoquinoline alkaloid, inhibits melanoma cancer cell migration by reducing the expressions of cyclooxygenase-2, prostaglandin E2 and prostaglandin E2 receptors, Carcinogenesis 32 (2011) 86–92.
[9] F. Qiu, Z. Zhu, N. Kang, et al., Isolation and identification of urinary metabolites of berberine in rats and humans, Drug Metab. Dispos. 36 (2008) 2159–2165.
[10] P. Rosignoli, R. Fabiani, A. Bartolomeo, et al., Genotoxic effect of bile acids on human normal and tumour colon cells and protection by dietary antioxidants and butyrate, Eur. J. Nutr. 47 (2008) 301–309.
[11] Q.Y. Li, W.N. He, L. Zhang, et al., Synthesis, anticancer activity, antimicrobial activities and bioavailability of berberine–bile acid analogues, Lett. Drug Des. Discov. 9 (2012) 573–580.
[12] H.A. Elrod, S.Y. Sun, Modulation of death receptors by cancer therapeutic agents, Cancer Biol. Ther. 7 (2008) 163–173.
[13] X. Wang, The expanding role of mitochondria in apoptosis, Genes Dev. 15 (2001) 2922–2933.
[14] S.A. Susin, H.K. Lorenzo, N. Zamzami, et al., Molecular characterization of mitochondrial apoptosis-inducing factor, Nature 397 (1999) 441–446.
[15] L.Y. Li, X. Luo, X.D. Wang, Endonuclease G is an apoptotic DNase when released from mitochondria, Nature 412 (2001) 95–99.
[16] S.A. Susin, E. Daugas, L. Ravagnan, et al., Two distinct pathways leading to nuclear apoptosis, J. Exp. Med. 192 (2000) 571–580.
[17] H.U. Simon, A. Haj-Yehia, F. Levi-Schaffer, Role of reactive oxygen species (ROS) in apoptosis induction, Apoptosis 5 (2000) 415–418.
[18] Q.Y. Li, W. Qiu, Q.Y. Zhu, et al., Camptothecin-20(s)-*O*-[*N*-(3′α,12′α-dihydroxy-24′-carbonyl-5′β- cholan)]-lysine, a novel camptothecin analogue, induces apoptosis towards hepatocellular carcinoma SMMC-7721 cells, Molecules 16 (2011) 7803–7814.
[19] X.N. Wang, X. Han, L.N. Xu, et al., Enhancement of apoptosis of human hepatocellular carcinoma SMMC-7721 cells through synergy of berberine and evodiamine, Phytomedicine 15 (2008) 1062–1068.
[20] M. Herrmann, H.M. Lorenz, R. Voll, et al., A rapid and simple method for the isolation of apoptotic DNA fragments, Nucleic Acids Res. 22 (1994) 5506–5507.
[21] M. Los, S. Wesselborg, K. Schulze-Osthoff, The role of caspases in development, immunity, and apoptotic signal transduction: lessons from knockout mice, Immunity 10 (1999) 629–639.
[22] C.M. Shih, W.C. Ko, J.S. Wu, et al., Mediating caspase-independent apoptosis by cadmium through mitochondria-ROS pathway in MRC-5 fibroblasts, J. Cell. Biochem. 91 (2004) 383–397.
[23] R.L. Cai, W. Meng, H.Y. Lu, et al., Segregation analysis of hepatocellular carcinoma in a moderately high-incidence area of east china, World J. Gastroenterol. 9 (2003) 2428–2432.
[24] T.J. Song, E.W. Ip, Y. Fong, Hepatocellular carcinoma: current surgical management, Gastroenterology 127 (2004) S248–S260.
[25] M. Thomas, Molecular targeted therapy for hepatocellular carcinoma, J. Gastroenterol. 44 (2009) 136–141.
[26] L.W. Gao, J. Zhang, W.H. Yang, et al., Glaucocalyxin A induces apoptosis in human leukemia HL-60 cells through mitochondria-mediated deathpathway, Toxicol. In Vitro 25 (2011) 51–63.